Gauche Effect in 1,2-Difluoroethane. Hyperconjugation, Bent Bonds, Steric Repulsion

Lionel Goodman,* Hongbing Gu, and Vojislava Pophristic†

Department of Chemistry and Chemical Biology, Wright and Rieman Laboratories, Rutgers, The State University of New Jersey, New Brunswick, New Jersey 08901

Received: August 17, 2004; In Final Form: November 24, 2004

Natural bond orbital deletion calculations show that whereas the gauche preference arises from vicinal hyperconjugative interaction between anti C−H bonds and C−F* antibonds, the cis C−H/C−F* interactions are substantial (∼25% of the anti interaction). The established significantly >60° FCCF dihedral angle for the equilibrium conformer can then be rationalized in terms of the hyperconjugation model alone by taking into account both anti interactions that maximize near 60° and the smaller cis interactions that maximize at a much larger dihedral angle. This explanation does not invoke repulsive forces to rationalize the 72° equilibrium conformer angle. The relative minimum energy for the trans conformer is the consequence of a balance between decreasing hyperconjugative stabilization and decreasing steric destabilization as the FCCF torsional angle approaches 180°. The torsional coordinate is predicted to be strongly contaminated by CCF bending, with the result that approximately half of the trans → gauche stabilization energy stems from mode coupling.

I. Introduction

Preference of 1,2-difluoroethane (DFE) for the gauche conformation (Figure 1a) over the eclipsed or trans structures (Figure 1b−d) is usually identified as the *gauche effect*. The existence of a gauche effect appears to have been first pointed out and given its name by Wolfe[1] in 1972. The gauche position in DFE can be considered as a step in rotation of one of the fluoromethyl groups around the C−C bond. Infrared, electron diffraction and microwave experiments,[2−5] dipole moment analyses,[6] and diverse theoretical calculations[7−24] have securely established a ∠FCCF dihedral angle near 71−72° (taking the F−F eclipsed position as 0°) for the stable equilibrium conformer. The energetic consequence of the gauche effect is frequently characterized as the energy difference between the equilibrium gauche and metastable trans conformers, $\Delta E_{T\rightarrow G}$. Experiment[2] and a plethora of computational investigations establish this to be close to −0.8 kcal/mol.

Examples of the gauche effect are found in many molecules (e.g., the hydrogen positions in hydrazine[25] and in hydrogen peroxide[26]), but disubstituted ethanes and in particular DFE have historically been considered the benchmark cases for understanding the origin of gauche structural preference. A number of attempts at its rationalization in DFE have been made,[7−12] the most cogent of these involves hyperconjugation.[7−9] Brunck and Weinhold,[8] by taking advantage of a feature of bond orbital theory that facilely allows the hyperconjugative interactions to be switched off, showed that the trans conformation becomes preferred when the these interactions are deleted. They argued that the most important interaction involves charge transfer from a nearly filled donor bonding orbital (C−H in DFE) anti to an almost vacant acceptor orbital (C−F* in DFE) involving the adjacent (vicinal) carbon. Because this interaction is maximized in the 60° orientation,[8] it preferentially stabilizes the gauche structure. Dipole−dipole repulsion is frequently invoked as the interaction that forces the dihedral FCCF angle beyond 60° predicted for DFE by the hyperconjugative model.

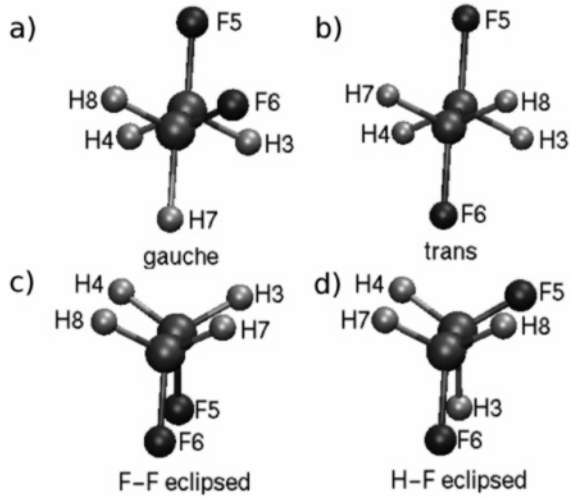

Figure 1. Difluoroethane conformers.

The hyperconjugation orbital overlap connection can be usefully expressed as donor−acceptor interactions between natural bond orbitals (NBOs).[27] The link between hyperconjugation and orbital overlap involving vicinal anti donor−acceptor stabilizing interactions as the determining factor for conformational preference provides a rationale for the gauche effect in general. It allows formulation of simple conformational rules to understand structural trends in ethane-like molecules.[8] Even so, challenges to the hyperconjugation model have appeared. Wiberg et al.[10,11] considered the effect of fluorine orientations on the strength of the central C−C bond. This model invokes the electrostatic pull of the highly electronegative fluorines to warp the C−C bond (see section VI) so that in the trans position the bond density is reduced in contrast to the greater overlap appropriate to the bent bond in the gauche position. The logical outcome is that the gauche conformer is stabilized relative to trans. Rablen et al.[9] carried out a clever test of the hypercon-

* Corresponding author. E-mail: goodman@rutchem.rutgers.edu.
† Present address: Department of Chemistry and Biochemistry, University of the Sciences in Philadelphia, Philadelphia, PA 19104.

10.1021/jp046290d CCC: $30.25
Published on Web 01/26/2005

TABLE 1: Difluoroethane Optimized Geometries (B3LYP/6-311+(d,p))[a]

coordinates	gauche (G)	trans (T)	difference (G − T)
R_{C-C}	1.505	1.519	−0.014
R_{C-F}	1.397	1.399	−0.0025
R_{C-H}	1.094	1.092	0.002
∠CCH	109.68	111.22	−1.54
∠CCF	110.82	108.05	2.77
∠FCH	107.75	108.21	−0.46
∠FCCH	120.71	118.53	2.18
∠FCCF	72.04	180.00	−108

[a] Energies in kcal/mol; bond lengths in Å; bond angles in degrees.

jugation model by examining the conformational preference of 1-fluoro-2-silyl ethane. Because the C−Si bond is known to be a much more vigorous donor than C−H, the trans conformation (where the anti C−Si bond acts as the donor to the C−F* orbital) should be soundly preferred over the gauche conformer (where only the C−H bonds are in the anti position). However, Rablen's calculations showed that although the trans conformer is preferred, it is only weakly so. In another recent computational study Trindle et al.[12] concluded that hyperconjugation, though significant for DFE, is not the sole determinant of conformational preference; electrostatic attractions play a role. Gauche preference is also predicted by the electrostatic attraction/repulsion scheme of molecular mechanics (MM).[13,14] However, even though on the surface MM does not seem to explicitly take into account hyperconjugation, its empirical parametrization may actually include orbital interactions, sub rosa.

The goal of this study is to use systematic deletion of electron transfers between selected bonds, lone pairs, and antibonds to pinpoint the orbital interactions responsible for the potential surface landscape. The equilibrium conformer populations and thermodynamic properties are determined by the properties of the minima on the potential surface. Therefore it is important to understand the role that cis C−H/C−F* interactions play in opening the preferred gauche FCCF dihedral angle from 60° required by the anti C−H/C−F* interaction to the larger angle found experimentally. NBO theory is used as a tool to analyze bond warping, and to analyze the effect of hyperconjugation and steric exchange repulsion on the gauche−trans potential surface. The FCCF dihedral angle dependence of the exchange repulsion allows insight into the origin of the metastable trans conformer. Its origin does not seem to have been explicitly addressed. Understanding the mechanism behind the energetics of the metastable trans conformer is no less important than understanding the cause of the 72° angle defining the gauche equilibrium conformer. Attention is also paid to skeletal relaxation effects, which we will show represent a significant portion of the trans-gauche stabilization energy, $\Delta E_{T\rightarrow G}$.

The all electron density functional, B3LYP/6-311G+(d,p), was used for geometry optimizations, trans → gauche stabilization energies, and deletion calculations. This level was chosen because it provides a reasonable trans → gauche energy difference, which agrees with the experimental value (Table 2), and a reasonable gauche structure as well as being computationally efficient. Because potential surfaces by their nature involve atomic position changes, attention was paid to basis set dependence by carrying out supplementary deletion calculations using extended HF/6-311G+(3df,2p) and B3LYP/6-311G+(2d,2p) basis sets. The only case that showed an important basis set dependence was deletion calculations involving the highly electronegative fluorine atom lone pairs. Steric exchange repulsion and hyperconjugation energies were calculated from both Hartree−Fock and DFT orbitals (see section IV) to increase the firmness of our conclusions. All calculations were carried out using Gaussian 98 version 11.0[28] with NBO 5.0.[29]

TABLE 2: Difluoroethane Trans → Gauche Energetics (kcal/mol)[a]

model	$E_T - E_G$[a]	exp $E_T - E_G$	barrier energy $E_B - E_G$[a]	exp barrier energy $E_B - E_G$
fully relaxed	0.82	0.8[b]	2.73	3.4[b]
rigid rotation[c]	0.42		2.69	

[a] B3LYP/6-311+G(d,p). [b] References 2 and 3. [c] Frozen at trans skeletal geometry.

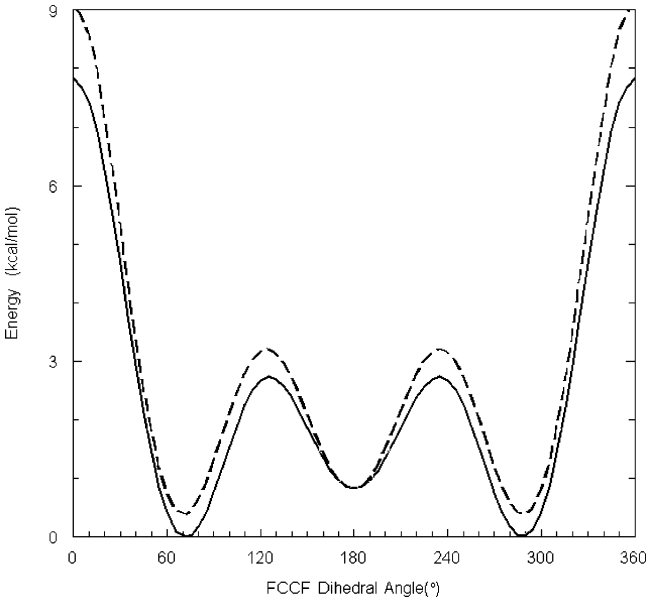

Figure 2. Difluoroethane potential curve in terms of FCCF dihedral angle rotation: (solid curve) fully relaxed; (dashed curve) rigid rotation, trans skeletal geometry frozen. 0°: F−F eclipsed. 120°: F−H eclipsed. 180°: metastable trans conformer. The energy zero is referenced to the 72° gauche equilibrium conformer.

II. Relaxation Effects

Trans → gauche rotation can be usefully decomposed into both a FCCF dihedral angle transforming rotation from the 180° trans geometry to the 72° equilibrium conformer and the nonrotational skeletal relaxations given in Table 1. Optimized geometries for the gauche and trans conformers (given in Table 1) show that there are three important skeletal relaxations: 1.5° ∠CCH and 0.014 Å C−C bond length decreases and a 3° ∠CCF increase. Insight into the role that these nonrotational coordinates play in the potential surface features, in particular the trans → gauche stabilization energy and G → T barrier, can be seen from two potential curves in terms of the FCCF dihedral angle, one with frozen trans skeletal geometry (dashed curve), the other obtained from global optimized geometries (full curve), given in Figure 2.

The features of both curves closely resemble each other, with three minima for 360° rotation and maxima at the 120° and 240° F−H eclipsed angles. However, there is a significant difference in $\Delta E_{T\rightarrow G}$. Frozen rotation reduces the trans−gauche stabilization energy (0.83 kcal/mol for the fully optimized potential curve) to 0.42 kcal/mol; however, the 2.7 kcal/mol fully relaxed gauche → trans barrier is virtually unchanged. We conclude that skeletal relaxation; i.e., the nonrotational phase space of the trans → gauche reaction path provides a major

TABLE 3: Difluoroethane T → G Partial Relaxation Energetics (kcal/mol)

relaxation	$\Delta E_G - \Delta E_T$
total[a]	−0.40
all bonds relaxed	−0.04
all angles[b] relaxed	−0.25
total methyl tilt	−0.13
∠CCH	−0.03
∠CCF	−0.08
CF−CF spread[c]	−0.15

[a] Difference between fully relaxed and rigid rotation energies, frozen at trans skeletal geometry. [b] Not including the two methyl tilt relaxations. [c] Twice ∠CCF relaxation.

contribution (i.e., nearly half) to the trans−gauche stabilization energy (see Table 2) and narrowing of the T → G barrier.

The specific skeletal coordinate changes causing the large nonrotational component of the trans → gauche stabilization energy are given in Table 3. Here only one bond length or angle is allowed to relax from its trans description; the other coordinates are frozen. Partially relaxed rotations allow insight into the roles that individual internal coordinates play in the trans → gauche process, and Table 3 shows that the paramount relaxations are the angular motions, accounting for most of the difference between the fully relaxed and rigid rotation descriptions of $\Delta E_{T\rightarrow G}$. Decomposition of the energy alteration caused by angular relaxation into individual relaxations reveals that two angular motions have a major effect with CCF angle opening the largest (note that there are four ∠CCH relaxations vs only two ∠CCF). It is noteworthy that the ∠CCF motion increases separation and alignment of the two C−F bonds in the gauche conformer (Table 1) consistent with relief of C−F/C−F dipole−dipole repulsion. The methyl tilt angle change also yields an important effect.

III. Hyperconjugation Model

The link between hyperconjugation and the gauche effect can be validated by carrying out two calculation schemes after removing all the electron charge transfers from bonds and lone pairs to antibond NBOs: (1) single point energy calculations at the 72° gauche and 180° trans geometries; (2) full geometry optimization for the potential curve with respect to ∠FCCF angle variation (Figure 3). The first set of calculations allows us to focus on the link between conformational preference and hyperconjugation without complication brought about by the skeletal changes. When all hyperconjugative interactions are switched off, the B3LYP/6-311+G(d,p) energy of the gauche conformer (in the single point scheme) is 7.6 kcal/mol higher than that of the trans, in accord with the 25 year old Brunck and Weinhold INDO orbital interaction removal calculations.[8] In the fully optimized NBO scheme the gauche conformational preference is also lost (Figure 3); i.e., the optimized FCCF angle strongly increases from the 72° gauche geometry to 129° (Figure 3 and Table 4). The 129° near-eclipsed geometry in this hypothetical DFE molecule is approximately 0.5 kcal/mol more stable than the trans geometry. Thus both the large ∠FCCF increase and G−T energy inversion provide validation for the important role that hyperconjugation plays in the gauche effect.

Removal of only the geminal hyperconjugations leaves the optimized DFE conformer essentially unchanged from gauche (Table 4). Thus geminal interactions, which include such bond/antibond charge transfers as C−H/C−C* and C−F/C−C* have little influence on the geometry of the preferred conformer. Removal of the sole geminal lone pair interaction, $lp(F_1) \rightarrow C_1-F_1^*$ also leads to only minor changes in conformational preference and insignificant deletion energies.

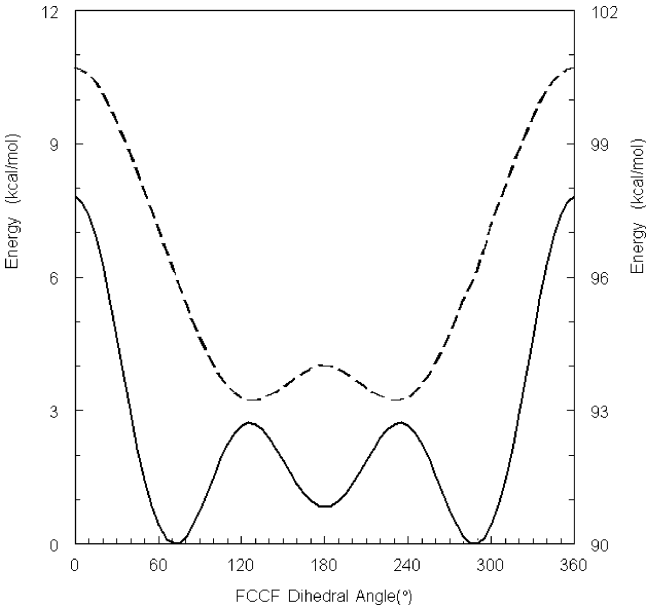

Figure 3. DFE fully optimized potential curves: (—) full Hamiltonian; (---) all hyperconjugative interactions deleted. Both curves have the same zero energy reference point as Figure 2.

TABLE 4: Difluoroethane Optimized Conformational Dependence on Hyperconjugative Interactions[a]

hyperconjugative model	optimized angle (deg)	preferred conformer
no deletion	72.0	gauche
no hyperconjugation	129.2	H−F eclipsed
no geminal hyperconjugation	70.2	gauche
no vicinal hyperconjugation	178.4	trans
no remote hyperconjugation	78.0	gauche

[a] All geometry optimizations carried out at the B3LYP/6-311+G(d,p) level.

When all vicinal hyperconjugations are removed, the triple minima potential of the real molecule is replaced by a single minimum representing the optimized trans geometry (Figure 4 and Table 4). The energy of the optimized trans conformer is now 3.8 kcal/mol lower than at the 72° gauche geometry. Of special interest is that this energy difference exceeds the 2.1 kcal/mol T−G energy difference when all hyperconjugations are removed.

Because of the importance of skeletal relaxation to the T−G stabilization energy (see section II), it is instructive to obtain hyperconjugation deletion energetics for rigid rotation (Table 5), thereby eliminating changes in skeletal bond lengths and angles. The same energetic pattern (i.e., vicinal interactions are more important than geminal ones) is shown in Table 5 for deletions with and without relaxation, indicating that the main factor in controlling orbital interactions is torsional rotation.

Figure 4 also shows the effect of deleting only the vicinal hyperconjugation interactions originating in bonds; those originating from lone pairs still remain. The similarity to the single minimum potential curve obtained with all vicinal hyperconjugations deleted is evident. Further, the energy of the trans conformer is 4.0 kcal/mol lower than that at the saddle point at the gauche geometry, close to that found for full vicinal interaction deletion (3.8 kcal/mol).

The potential curve for deletion of only the vicinal hyperconjugation interaction originating from lone pairs (Figure 4) was calculated with the saturated polarization basis set, B3LYP/6-311G+(3df,2p), as discussed in section I. The curve is strikingly different from deletion of only vicinal hyperconju-

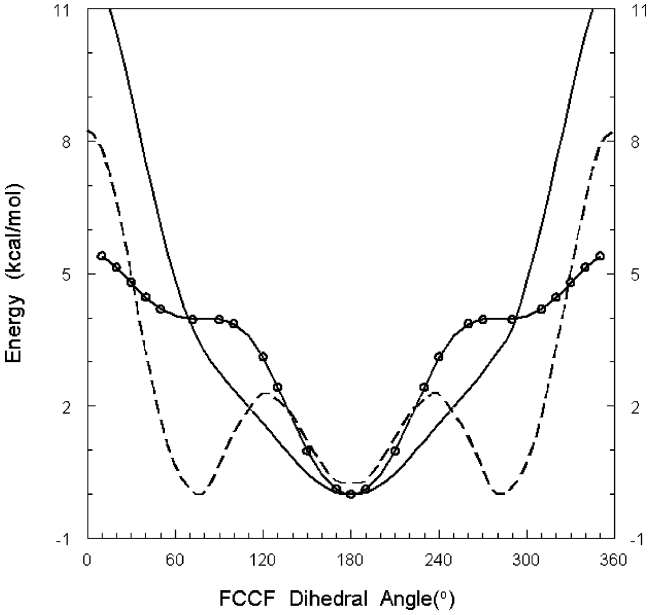

Figure 4. Potential curves with various vicinal hyperconjugative interaction categories deleted: (—) all vicinal hyperconjugative interactions deleted; (○) only vicinal bond interactions deleted; (---) only vicinal lone pair interactions deleted. All curves are fully optimized after specified deletions with exception of dashed single point calculation curve. The energy zero has been arbitrarily set at the minimum energy of each curve.

TABLE 5: Difluoroethane Relaxation Effect on Energetics of Hyperconjugative Deletions (kcal/mol)[a]

hyperconjugative model	FR[b]	RR[c]	FR/full Hamiltonian[d]
no deletion	0.82	0.42	0.82
no hyperconjugation	−2.29	−3.88	−7.56
no geminal hyperconjugation	−1.55	−2.05	−2.09
no vicinal hyperconjugation	−3.76	−7.04	−11.18

[a] Total energy difference, $E^{trans} - E^{gauche}$, after designated deletions. [b] Geometries fully optimized after deletion. [c] Single point calculation at 72° and 180° from frozen trans geometry without deletion. [d] Single point calculations at 72° and 180° using optimized 72° and 180° geometries without deletion.

TABLE 6: Difluoroethane Conformational Dependence on Vicinal Hyperconjugative Interactions[a]

hyperconjugative model	optimized angle (deg)	preferred conformer
no vicinal C_1-H/C_2-F^*	180.0	T
no vicinal C_1-H/C_2-H^*	78.4	G
no vicinal C_1-F/C_2-H^*	72.3	G
no vicinal C_1-F/C_2-F^*	79.5	G

[a] All geometry optimizations carried out at the B3LYP/6-311+G(d,p) level.

gations originating in bonds. It resembles the triple minimum signature of the real molecule with the principal and secondary minima near the same dihedral angles.

The clear conclusion obtained from Figure 4 and Tables 4 and 5 is that vicinal hyperconjugation interactions originating in bonds control the gauche effect. We note that the skeletal changes reported in Table 1 have little effect on this conclusion. Further, conformational preferences given in Table 6 indicate that it is the C_1-H/C_2-F^* interactions that are the most important ones. They are the only vicinal bond/antibond electron transfers whose deletion causes switching of the preferred gauche conformation to trans. This comes as no surprise because they represent charge transfer from a C−H donor bond to a strongly electron-accepting C−F* antibond. Deletion of all other vicinal bond interactions retains the gauche conformer as the preferred geometry.

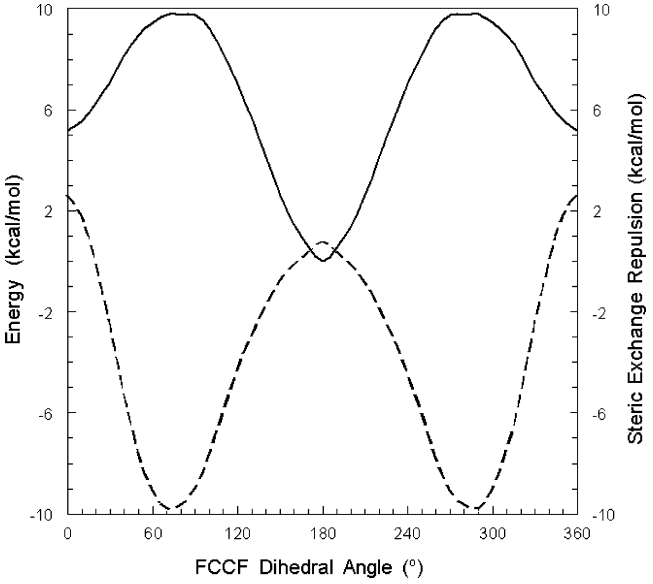

Figure 5. FCCF dihedral angle variation of B3LYP/6-311+G(d,p) steric exchange repulsion (—, right-hand scale), potential curve for a hypothetical DFE molecule with steric exchange repulsion removed (---, left-hand scale). The energy zero for the steric repulsion curve is arbitrarily taken at the 180° trans geometry.

As a final note, removal of remote hyperconjugative interactions (i.e., $lp(F_1)/C_2-H^*$ or $lp(F_1)/C_2-F^*$) only slightly alters the preferred dihedral angle of the gauche conformer (Table 4).

IV. Steric Repulsion Model

Steric repulsion is classically defined as the effect of Pauli exchange repulsion, a short-range force, which spatially separates pairs of electrons. Orthogonalization introduces nodes that preserve the Pauli exclusion principal by introducing kinetic energy pressure that opposes inter penetration of matter.[30] The Weisskopf view of steric repulsion is the conceptual foundation of NBO steric analysis.[29,31] Because orbital orthogonalization is a consequence of antisymmetrization, an appreciation of total steric exchange repulsion for a given molecular geometry can be obtained from the energy difference between orthogonal natural localized molecular orbital (NLMOs) and nonorthogonal preorthogonal natural localized molecular orbital (PNLMOs) descriptions of the molecular wave function.[32] The PNLMOs and NLMOs are closely related to PNBOs and NBOs with somewhat different localizations designed to improve exchange repulsion estimates. To assess the effect of correlation on the exchange repulsion, we calculated the steric exchange repulsion in two ways: (1) with the full correlation potential (B3LYP/6-311G+(d,p)) and (2) with the correlation part of B3LYP set equal to zero. Both calculated exchange repulsion-dihedral angle curves (solid line in Figure 5) are similar, showing a maximum at or near the 72° gauche FCCF dihedral angle and a pronounced minimum at 180°, the trans angle. Because there are only minor differences in the landscape from the two ways of calculating the exchange repulsion−dihedral angle variation, we conclude that the exchange repulsion is not correlation sensitive.

The dashed curve represents the potential curve for a hypothetical DFE molecule with exchange repulsion removed. The striking feature of the hypothetical molecule potential curve in Figure 5 is that the optimal 72° FCCF dihedral angle remains the same regardless of whether steric repulsion is present or

not. Moreover, it exhibits no minimum at the trans FCCF dihedral angle. As seen from comparison of Figures 2 and 5, the effect of removing steric exchange repulsion is to greatly increase the gauche−trans energy difference, a consequence of exchange repulsion destabilization of the gauche conformer.

The important conclusion is that steric exchange repulsion plays a major if not determining role in stabilizing the metastable 180° trans conformer. However, Figure 5 also shows that exchange repulsion does not play a significant role in forming the DFE gauche conformational preference because it is strongly destabilizing at the gauche geometry. The role of the nonrotational coordinates in exchange repulsion can be obtained by comparing fully relaxed and rigid rotation repulsion curves. The features discussed above are qualitatively similar when skeletal relaxation is frozen out. Thus the main conclusion of the exchange repulsion calculations, that it plays a key role in stabilizing the trans conformer, is independent of the coupling of torsion to other modes, even though the energetic preference for the gauche conformer is affected by such coupling.

V. Bent Bond Model

The NBO procedure allows an examination of the role of bent bonds in the gauche effect. In NBO theory, a bent bond is described as the angular deviation of the two natural hybrid atomic orbitals (NHOs) making up the bond from the centerline of the bond. The deviation is then controlled by the details of the NHO polarization. The DFT calculated carbon NHO deviations from the carbon−carbon nuclear centerline for the gauche conformer is 2.1° (bent toward each other) compared to 1.7° (bent away from each other) for trans.

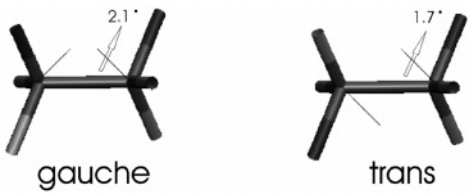

This result supports Wiberg's reasoning[10,11] that the electronegative fluorine atom bends the C−C bond to different degrees and with different senses in the two conformers. The NHO deviations are also comparable to the bond path[33] ones calculated by Wiberg et al. (2.8° for gauche and 2.15° for trans).[10] However, the calculated overlap integral between the gauche NHOs, 0.789 compared to 0.786 for trans is increased by less than 0.4% for the fully relaxed T → G path and only by a minuscule amount for the rigid rotation path. Nearly all of this overlap integral change is linked to the decrease in C−C bond length, and not to the bond bending.

An attempt was made to "freeze out" bond bending by transferring the carbon NHOs from the trans conformer to the gauche one. The overlap increase found for the transferred NHOs in fully relaxed T → G rotation is now reduced to only 0.001 from 0.003 for the untransferred NHOs. A parallel rigid rotation calculation reduces the overlap increase by almost the same magnitude. The results of the two calculations (transferred and untransferred NHOs) suggest that the overlap increase due to bond bending is too small to account for a significant portion of the ∼1 kcal/mol preferential stabilization of the gauche conformer.

VI. Discussion

The geometry inversion that occurs in the absence of electron transfer involving bond interactions (discussed in section IV (see Figures 3 and 4)) solidly establishes the link between these vicinal hyperconjugative interactions and the gauche effect. Figure 6 isolates the intuitively satisfying C−H/C−F* charge transfers from the other bond interactions. The solid line represents the potential curve with only the C_1−H/C_2−F* charge transfers removed; all other hyperconjugative interactions remain. This curve with its single 180° minimum and inflection near 70° resembles the no-bond vicinal interaction curve of Figure 4. Alternatively, the problem can be viewed through the dashed curve in Figure 6, which inverts the deletions associated with the solid curve by keeping only the C_1−H/C_2−F* interactions with all other hyperconjugative charge transfers switched off. This potential curve (exhibiting minima near 95° and 260°) is noteworthy because the minimum at the 180° trans geometry, characteristic of the potential for the real molecule, is absent.

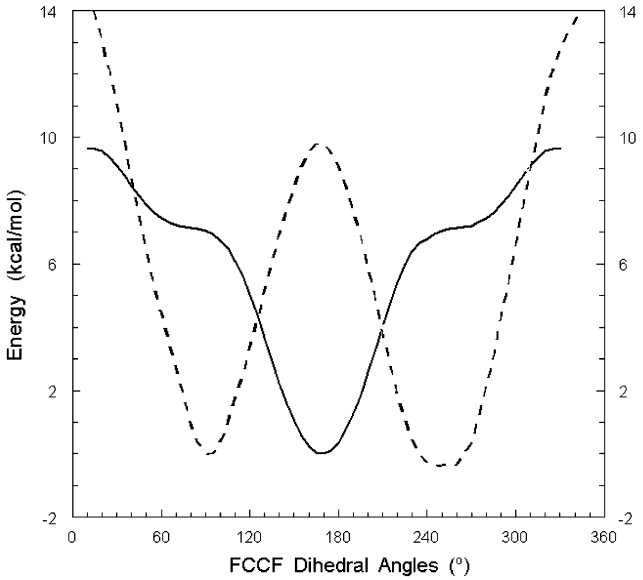

Figure 6. Fully optimized potential curves obtained: when only the C_1−H/C_2−F* interactions are removed (—); when only the C_1−H/C_2−F* interactions are retained with all other interactions expunged (---). Energy zero is arbitrarily taken at minimum of (---) curve.

TABLE 7: C_1−H/C_2−F* Second-Order Perturbation Hyperconjugative Interaction Energies (kcal/mol) and Overlap Integrals

	gauche		trans	
hyperconjugative model	$E(2)$	$S_{i,j}$	$E(2)$	$S_{i,j}$
anti C_1−H/C_2−F*	4.74	0.197	0.53	0.056
cis C_1−H/C_2−F*	1.38	0.090	0.53	0.056

The C_1−H/C_2−F* interactions can be further parsed into the individual C_1−H_3/C_2−F* and C_1−H_4/C_2−F* interactions, involving the two possible types of C−H bonds: anti (C_1−H_3) and cis (C_1−H_4) (see Figure 1). The second-order perturbation energies for these two C−H bond interaction categories given in Table 7 show that the anti C_1−H/C_2−F* perturbation energy, 4.74 kcal/mol in the gauche conformer, is more than triple that for the cis (1.38 kcal/mol), in conformity with the orbital overlaps shown in Figure 7. Overlap of the main lobe of the anti oriented C_1−H orbital with the back lobe of the C_2−F* antibond is much greater than for the cis oriented C_1−H. This difference vanishes in the trans geometry, where both C_1−H bonds become cis and equivalent.

For intermediate values of the FCCF dihedral angle between 72° and 180°, the two bond NBOs take on each other's orientational character; e.g., the overlap integral for the cis

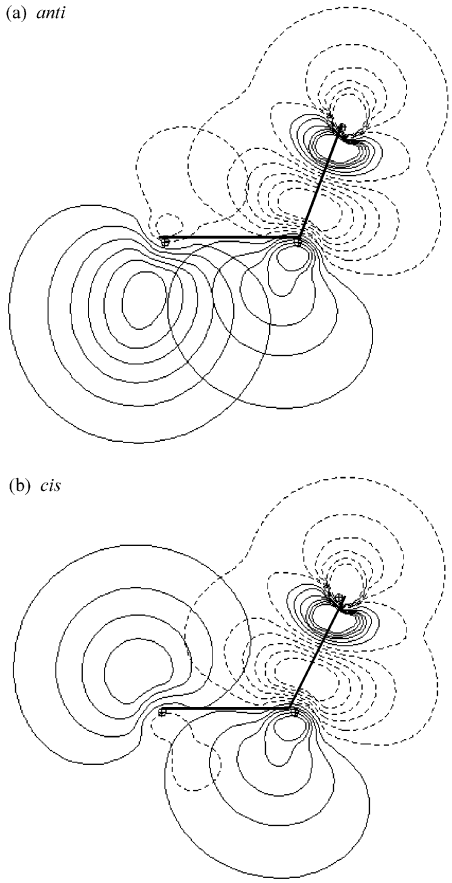

Figure 7. Anti C−H/C−F* (a) and cis C−H/C−F* orbital (b) overlaps, showing the greater overlap of the main lobe of the anti orbital C−H bond with the back lobe of the C−F* antibond. The orbital contours are shown in the CCF plane.

originating interaction C_1-H_4/C_2-F^* maximizes at 120° compared to 60° for anti. At the 120° geometry, the main lobe of the C_1-H_4 bond overlaps the main lobe of the C−F* antibond much more strongly than at the gauche geometry. (It needs to be emphasized that the anti and cis designations lose their meaning as the dihedral angle advances toward 180°.)

As an alternate approach to the DFT orbital interactions described in the preceding sections, we repeated the deletion calculations using HF orbitals (HF/6-311++G(3df,2p)) with the same qualitative results as the DFT ones. The raison d'etra for the HF calculations is that the DFT virtual orbitals are defined in the field of the molecular ions and the HF ones are defined in the field of molecules.

VII. Conclusions

The gauche effect has been used for decades to explain various structural characteristics and chemical phenomena. Despite the widespread use of the term, its origin and thus the underlying mechanism is not fully comprehended. In this work, we analyze several possible mechanisms (found to be important in studying structural effects) at the same footing using high level ab intio calculations. These calculations allow us to reach comprehensive explanations for both the origin of the gauche effect in DFE and its deviation from the intuitive 60° angle.

Our deletion calculations provide convincing validation that the C−H bond originating hyperconjugative interactions supply the backbone for the gauche effect in DFE, and that participation of both cis and anti C− H/C−F* interactions rationalize the well established >60° FCCF dihedral angle inherent to the equilibrium conformer. The existence of a metastable trans conformer in DFE is linked to lower steric exchange repulsion at the trans geometry. The metastable trans conformer, in this view, arises from competition between decreasing hyperconjugative stabilization and steric exchange repulsion as the FCCF dihedral angle increases. An additional conclusion is that approximately half of the trans → gauche stabilization energy stems from mode coupling.

Our rationalization of the >60° dihedral angle in the equilibrium conformer does not require a repulsive interaction (e.g., dipole−dipole repulsion); however, it does not logically eliminate electrostatic repulsions from playing a possible role either. It also allows an understanding of the surprising result of Rablen's conformational study of 1-fluoro-2-silylethane,[9] concluding that the trans conformer is only weakly preferred over gauche. According to our conclusion, account must be taken of *both* anti and cis donor orbitals in understanding gauche−trans potential surfaces. A cis C−Si/C−F* interaction is expected to be more favorable than a cis C−H/C−F* one, weakening the strong trans conformer preference when the anti interactions are considered alone.

An overarching conclusion of this study combined with previous work on several classes of organic molecules[40] (see, e.g., refs 8, 9, 12, 31, and 34−39) is that delocalization effects are critical in conformational preference in a wide range of molecules. The consequence is that the traditional approach involving only steric repulsion in dealing with structural issues in chemistry is inadequate. Delocalization needs to be considered at the same level of importance.

Acknowledgment. As part of his senior thesis, Jon Feenstra carried out preliminary calculations on difluoroethane, which provided a helpful guide for the study reported here. We thank Frank Weinhold for helpful comments on the manuscript.

References and Notes

(1) Wolfe, S. *Acc. Chem. Res.* **1972**, *5* (3), 102−111.
(2) Durig, J. R.; Liu, J.; Little, T. S.; Kalasinsky, V. F. *J. Phys. Chem.* **1992**, *96* (21), 8224−8233.
(3) Craig, N. C.; Chen, A.; Suh, K. H.; Klee, S.; Mellau, G. C.; Winnewisser, B. P.; Winnewisser, M. *J. Phys. Chem. A* **1997**, *101* (49), 9302−9308.
(4) Fernholt, L.; Kveseth, K. *Acta Chem. Scand., A: Phys. Inorg. Chem.* **1980**, *A34* (3), 163−170.
(5) Takeo, Harutoshi; Matsumura, Chi; Morino, Yonezo. *J. Chem. Phys.* **1986**, *84* (8), 4205−4210.
(6) Goodwin, A. R. H.; Morrison, G. *J. Phys. Chem.* **1992**, *96* (13), 5521−5526.
(7) Radom, L.; Lathan, W. A.; Hehre, W. J.; Pople, J. A. *J. Am. Chem. Soc.* **1973**, *95*, 693−698.
(8) Brunck, T. K.; Weinhold, F. *J. Am. Chem. Soc.* **1979**, *101* (7), 1700−1709.
(9) Rablen, P. R.; Hoffmann, R. W.; Hrovat, D. A.; Borden, W. T. *J. Chem. Soc., Perkin Trans. 2*: **1999**, No. 8, 1719−1726.
(10) Wiberg, K. B.; Murcko, M. A.; Laidig, K. E.; MacDougall, P. J. *J. Phys. Chem.* **1990**, *94* (18), 6956−6959.
(11) Wiberg, K. B. *Acct. Chem. Res.* **1996**, *29* (5), 229−234.
(12) Trindle, C.; Crum, P.; Douglass, K. *J. Phys. Chem. A* **2003**, *107* (32), 6236−6242.
(13) Box, Vernon G. S.; Box, Lynda L. *J. Mol. Struct.* **2003**, *649* (1−2), 117−132.
(14) Chen, K.-H.; Walker, G. A.; Allinger, N. L. *THEOCHEM* **1999**, *490*, 87−107.
(15) Engkvist, O.; Karlstroem, G.; Widmark, P.-O. *Chem. Phys. Lett.* **1997**, *265* (1, 2), 19−23.
(16) Papasavva, Stella; Illinger, Karl H.; Kenny, Jonathan E. *J. Phys. Chem.* **1996**, *100* (24), 10100−10110.
(17) Martell, J. M.; Boyd, R. J.; Shi, Z. *J. Phys. Chem.* **1993**, *97* (28), 7208−7215.
(18) Topol, I. A.; Burt, S. K. *Chem. Phys. Lett.* **1993**, *204* (5−6), 611−616.

(19) Dixon, D. A.; Matsuzawa, N.; Walker, S. C. *J. Phys. Chem.* **1992**, *96* (26), 10740−10746.
(20) Dixon, D. A.; Smart, B. E. *J. Phys. Chem.* **1988**, *92* (10), 2729−2733.
(21) Wiberg, K. B.; Murcko, M. A. *J. Phys. Chem.* **1987**, *91* (13), 3616−3620.
(22) Miyajima, Takashi; Kurita, Yasuyuki; Hirano, Tsuneo. *J. Phys. Chem.* **1987**, *91* (15), 3954−3959.
(23) Smits, G. F.; Krol, M. C.; Van Kampen, P. N.; Altona, Cs. *THEOCHEM* **1986**, *32* (3−4), 247−253.
(24) Radom, L.; Baker, J.; Gill, P. M. W.; Nobes, R. H.; Riggs, N. V. *J. Mol. Struct.* **1985**, *126*, 271−290.
(25) Werpetinski, K. S.; Cook, M. *J. Chem. Phys.* **1997**, *106* (17), 7124−7138.
(26) Wolfe, S.; Rauk, A.; Tel, L. M.; Csizmadia, I. G. *J. Chem. Soc. B: Phys. Org.* **1971**, *1*, 136−145.
(27) Weinhold, F. In *The Encyclopedia of Computational Chemistry*; P. v. R. Schleyer, N. L. Allinger, T. Clark, J. Gasteiger, P. A. Kollman, H. F. Schaefer III, P. R. Schreiner, Eds.; John Wiley & Sons: Chichester, U.K., 1998; pp 1792−1811.
(28) Frisch, M. J.; Trucks, G. H.; Schlegel, H. B.; Scuseria, G. E.; Robb, M. A.; Cheeseman, J. R.; Zakrzewski, V. G.; Montgomery, J. A.; Stratmann, R. E.; Burant, J. C.; Dapprich, S.; Millam, J. M.; Daniels, A. D.; Kudin, K. N.; Strain, M. C.; Farkas, O.; Tomasi, J.; Barone, V.; Cossi, M.; Cammi, R.; Mennucci, B.; Pomelli, C.; Adamo, C.; Clifford, S.; Ochterski, J.; Petersson, G. A.; Ayala, P. Y.; Cui, Q.; Morokuma, K.; Malick, D. K.; Rabuck, A. D.; Raghavachari, K.; Foresman, J. B.; Cioslowski, J.; Ortiz, J. V.; Stefanov, B. B.; Liu, G.; Liashenko, A.; Piskorz, P.; Komaromi, I.; Gomperts, R.; Martin, R. L.; Fox, D. J.; Keith, T.; Al-Laham, M. A.; Peng, C. Y.; Nanayakkara, A.; Gonzalez, C.; Challacombe, M.; Gill, P. M. W.; Johnson, B. G.; Chen, W.; Wong, M. W.; Andres, J. L.; Head-Gordon, M.; Replogle, E. S.; Pople, J. A. *Gaussian 98*; Gaussian, Inc.: Pittsburgh, PA, 1998.
(29) Glendening, E. D.; Badenhoop, J. K.; Reed, A. E.; Carpenter, J. E.; Weinhold, F. *NBO 4.0* and *NBO 5.0*; Theoretical Chemistry Institute, University of Wisconsin: Madison, 1996 and 2002.
(30) Weisskopf, V. F. *Science* **1975**, *187*, 605−612.
(31) Badenhoop, J. K.; Weinhold, F. *J. Chem. Phys.* **1997**, *107* (14), 5406−5421, 5422.
(32) Reed, A. E.; Weinhold, F. *J. Chem. Phys.* **1985**, *83* (4), 1736−1740.
(33) Runtz, G. R.; Bader, R. F. W.; Messer, R. R. *Canad. J. Chem.* **1977**, *55* (16), 3040−3045.
(34) Pophristic, V.; Goodman, L. *Nature* **2001**, *411* (6837), 565−568.
(35) Pophristic, V.; Goodman, L. *J. Phys. Chem. A* **2003**, *107*, 3538.
(36) Pophristic, V.; Goodman, L.; Gorb, L.; Leszczynski, J. *J. Chem. Phys.* **2002**, *116*, 7049.
(37) Pophristic, V.; Goodman, L. *J. Phys. Chem.* **2002**, *106* (8), 1642−1646.
(38) Wilcox, C. F.; Bauer, S. H. *J. Mol. Struct. (THEOCHEM)*, **2003**, *625*, 1−8.
(39) Wolfe, S.; Shi, Z. *Isr. J. Chem.* **2000**, *40* (3−4), 343−355.
(40) These molecules range from the simple hydrocarbon molecules and fluoro-substituted propanes[41] to aromatic aldehydes and complex sugars.
(41) Goodman, L.; Sauers, R. Unpublished work.